Copyright © 1998 by the Genetics Society of America

Gain-of-Function Mutations in the *Caenorhabditis elegans lin-1* ETS Gene Identify a C-Terminal Regulatory Domain Phosphorylated by ERK MAP Kinase

Dave Jacobs,* Greg J. Beitel,†,[1] Scott G. Clark,†,[2] H. Robert Horvitz† and Kerry Kornfeld*

**Department of Molecular Biology and Pharmacology, Washington University School of Medicine, St. Louis, Missouri 63110 and †Howard Hughes Medical Institute, Department of Biology, Massachusetts Institute of Technology, Cambridge, Massachusetts 02139*

Manuscript received March 31, 1998
Accepted for publication April 30, 1998

ABSTRACT

Genetic analysis of *lin-1* loss-of-function mutations suggests that *lin-1* controls multiple cell-fate decisions during *Caenorhabditis elegans* development and is negatively regulated by a conserved receptor tyrosine kinase-Ras-ERK mitogen-activated protein (MAP) kinase signal transduction pathway. LIN-1 protein contains an ETS domain and presumably regulates transcription. We identified and characterized six gain-of-function mutations that define a new class of *lin-1* allele. These *lin-1* alleles appeared to be constitutively active and unresponsive to negative regulation. Each allele has a single-base change that affects the predicted C terminus of LIN-1, suggesting this region is required for negative regulation. The C terminus of LIN-1 was a high-affinity substrate for Erk2 *in vitro*, suggesting that LIN-1 is directly regulated by ERK MAP kinase. Because *mpk-1* ERK MAP kinase controls at least one cell-fate decision that does not require *lin-1*, our results suggest that MPK-1 contributes to the specificity of this receptor tyrosine kinase-Ras-MAP kinase signal transduction pathway by phosphorylating different proteins in different developmental contexts. These *lin-1* mutations all affect a four-amino-acid motif, FQFP, that is conserved in vertebrate and Drosophila ETS proteins that are also phosphorylated by ERK MAP kinase. This sequence may be a substrate recognition motif for the ERK subfamily of MAP kinases.

INTERCELLULAR signaling is one of the primary mechanisms used to establish patterns of cell fates during development. We are analyzing intercellular signaling during the development of the vulva of the nematode *Caenorhabditis elegans*, because signaling events between easily visualized cells have been well defined and mutations that disrupt vulval development can be readily identified and characterized (reviewed by Horvitz and Sternberg 1991; Sundaram and Han 1996; Kornfeld 1997). Our goals are to identify the molecules that transduce signals and control cell fates, elucidate the interactions among these molecules, and understand how these molecules function in a developing animal.

In third larval stage hermaphrodites, six ventral epidermal blast cells called P3.p, P4.p, P5.p, P6.p, P7.p, and P8.p (Pn.p cells) lie along the anterior-posterior axis. Each of these Pn.p cells can adopt any of three distinct fates: the primary (1°) vulval cell fate (eight descendants), the secondary (2°) vulval cell fate (seven descendants), or the nonvulval tertiary (3°) cell fate (two descendants) (reviewed by Horvitz and Sternberg 1991). The anchor cell of the somatic gonad signals P6.p to adopt the 1° fate. P6.p signals P5.p and P7.p to adopt the 2° fate by activating *lin-12*, which is similar to the receptor Notch; the anchor cell signal may also promote the 2° fate. P3.p, P4.p, and P8.p receive neither signal and adopt the 3° fate. The 22 descendants of P5.p, P6.p, and P7.p generate the vulva, a specialized epidermal structure used for egg laying.

The anchor cell and P6.p communicate using a highly conserved signal transduction pathway that includes the *lin-3* ligand, which is similar to epidermal growth factor; the *let-23* receptor tyrosine kinase (RTK); the *sem-5* adaptor protein; *let-60* Ras; *lin-45* Raf; *mek-2* mitogen-activated protein (MAP) kinase kinase; and *mpk-1*/*sur-1* ERK MAP kinase (reviewed by Kornfeld 1997). A mutation that reduces the activity of one of these genes causes all six Pn.p cells to adopt the nonvulval 3° fate, resulting in a vulvaless (Vul) phenotype. By contrast, a constitutively active form of one of these genes causes all six Pn.p cells to adopt the 1° or 2° vulval fate, resulting in a multivulva (Muv) phenotype characterized by ectopic patches of vulval tissue. This signaling pathway functions at multiple times during development and is required for larval viability, hermaphrodite fertility, and other processes. RTK-Ras-MAP kinase signaling pathways have been conserved during evolution, and these pathways control a variety of cell-fate decisions during Drosophila and vertebrate development (reviewed by Dickson and Hafen 1994).

Corresponding author: Kerry Kornfeld, Department of Molecular Biology and Pharmacology, Washington University School of Medicine, Campus Box 8103, 660 S. Euclid Ave., St. Louis, MO 63110. E-mail: kornfeld@pharmdec.wustl.edu

[1]*Present address:* Department of Biochemistry, Stanford University School of Medicine, Stanford, CA 94305.

[2]*Present address:* Molecular Neurobiology Program, Skirball Institute, New York University Medical Center, New York, NY 10016.

These observations raise two important questions: How do these signaling proteins cause a change in cell fate, and how does this conserved signaling pathway specify different cell fates in different developmental contexts? MAP kinases, a family of serine/threonine-specific protein kinases, may be important for both processes (reviewed by Davis 1995; Treisman 1996). Activated MAP kinase can translocate into the nucleus *in vivo* and phosphorylate a variety of proteins *in vitro*, including transcription factors. This activity may be how this signaling system affects gene expression and cell fate. Furthermore, it is possible that a given MAP kinase can phosphorylate different proteins in different developmental contexts and in this way contribute to the specificity of the response. These possibilities have not been carefully tested, because only a few proteins have been shown to be MAP kinase substrates *in vivo* and because the basis for MAP kinase recognition of particular substrates remains to be determined.

Genetic experiments revealed that *lin-1* is an important regulator of multiple cell-fate decisions in *C. elegans* and suggested that *lin-1* functions downstream of *mpk-1* ERK MAP kinase. A *lin-1* loss-of-function (lf) mutation causes all six Pn.p cells to adopt vulval cell fates, even in the absence of the activity of the RTK-Ras-MAP kinase signaling pathway (Horvitz and Sulston 1980; Sulston and Horvitz 1981; Ferguson and Horvitz 1985; Ferguson *et al.* 1987; Lackner *et al.* 1994; Beitel *et al.* 1995). A *lin-1(lf)* mutation bypasses the requirement for the activity of the RTK-Ras-MAP kinase pathway to promote larval viability (Han *et al.* 1990; Kornfeld *et al.* 1995a,b; Sundaram and Han 1995). These observations suggest that the major function of the RTK-Ras-MAP kinase signaling pathway in at least two developmental processes is to regulate *lin-1* negatively.

lin-1 is predicted to encode a 441-amino-acid protein that contains an ETS domain (Beitel *et al.* 1995). The ETS domain appears to be required for *lin-1* function, because mutations that alter conserved residues in the ETS domain greatly reduce or eliminate *lin-1* activity. The ETS domains of related proteins bind DNA, and many ETS proteins are transcription factors (reviewed by Wasylyk *et al.* 1993). These observations suggest but do not prove that LIN-1 binds DNA and regulates transcription. ETS proteins are involved in a variety of processes, and several appear to be regulated by RTK-Ras-MAP kinase pathways, such as vertebrate Elk-1 and Drosophila Aop (*anterior open*; previously known as *yan* or *pok*) (reviewed by Treisman 1996).

To investigate the interaction between LIN-1 and ERK MAP kinase, we used biochemical and genetic experiments to show that the C terminus of LIN-1 is a substrate for Erk2 and is important for negative regulation of LIN-1 by the RTK-Ras-ERK MAP kinase pathway. Furthermore, we identified a C-terminal region of LIN-1 that is similar to the C box, a conserved domain present in the C-terminal regions of ETS proteins in the Elk subfamily (Treisman 1994). Our analysis suggests that the conserved elements of the C box are multiple S/TP motifs that are potential MAP kinase phosphorylation sites and an FQFP motif that we postulate to be a recognition sequence for ERK MAP kinase.

MATERIALS AND METHODS

General methods and strains: *C. elegans* strains were cultured as described by Brenner (1974) and were grown at 20° unless otherwise noted. The wild-type strain and parent of all mutant strains was N2. Unless otherwise noted, mutations used in this study are described by Riddle *et al.* (1997) and are as follows. LGI: *unc-54(r293)*; *smg-1(r861)*. LGII: *lin-8(n111)*; *lin-31(n1053)*. LGIV: *lin-1(n1761, n1790, n1855, n2515, n2525, ky54)* (this study); *lin-1(sy254, e1777)*; *dpy-9(e12); dpy-13(e184)*; *dpy-20(e1282)*; *ced-2(e1752)*; *unc-17(e113)*; *unc-24(e138)*; *unc-33(e204)*; *let-60(n1046gf)*; *nT1n754*; *mDp1* (Rogalski and Riddle 1988). LGV: *dpy-11(e224)*; *unc-41(n2913)*. LGX: *lin-15(n765ts)*. We used standard techniques to separate the *lin-1(gf)* mutations from the *let-60(gf)* or the *lin-15(lf)* mutation and to generate double mutants (Brenner 1974). We used DNA sequencing to confirm that *n1855*, *n2515*, and *n2525* were present on recombinant chromosomes that contained *let-60(+)* and the linked marker *dpy-13*.

Identification of *lin-1(gf)* mutations: We previously described a screen for suppressors of the *let-60(gf)* Muv phenotype (Lackner *et al.* 1994; Kornfeld *et al.* 1995a,b). In brief, we mutagenized *let-60(n1046gf)* hermaphrodites with ethyl methanesulfonate (EMS), placed 2794 F_1 self-progeny on separate Petri dishes, and examined the F_2 self-progeny for non-Muv animals at 22.5°. We identified 33 independently derived mutations that reduced the penetrance of the Muv phenotype from 93% to less than 10%, including the *lin-1* alleles *n2515* and *n2525*. In a related screen that we described previously (Beitel *et al.* 1990), we mutagenized *lin-8(n111); let-60(gf)* hermaphrodites with EMS and picked non-Muv F_1 self-progeny to separate Petri dishes at 25°. Ten extragenic mutations identified in this screen met the criteria described above, including *lin-1(n1855)*. We also previously described a screen for suppressors of the *lin-15(lf)* Muv phenotype (Beitel *et al.* 1990; Clark *et al.* 1992, 1993). In brief, we mutagenized *lin-15(n765ts)* hermaphrodites with EMS and examined the progeny of 38,000 F_1 animals for non-Muv animals. *lin-1(n1761)* and *lin-1(n1790)* were isolated in this screen. We isolated *ky54* as a vulva-defective animal in a screen for mutants affecting an unrelated phenotype after mutagenizing N2 animals with EMS (S. G. Clark and C. Bargmann, unpublished results).

Genetic mapping and complementation tests: The suppression of the *let-60(gf)* Muv phenotype caused by *n1855*, *n2515*, and *n2525* displayed linkage to *let-60* and *dpy-20* on chromosome *IV* (data not shown). To investigate complementation between these mutations, we scored the penetrance of the Muv phenotype in self-progeny from hermaphrodites with the following genotypes: *n1855 let-60(n1046)/n2515 let-60(n1046)* (0%, $n = 120$); *n1855 let-60(n1046)/n2525 let-60(n1046)* (2%, $n = 123$). The suppression of the *let-60(gf)* Muv phenotype caused by these three mutations was semidominant; for example, *+let-60(n1046)/n2525 let-60(n1046)* animals were 15% Muv. However, these mutations partially complemented several other suppressor mutations located on chromosome *IV* (data not shown) and thus appeared to define one complementation group. We used a three-factor cross and a four-factor cross to map the suppression of the *let-60(gf)* Muv phenotype caused by *n1855* more precisely. Of uncoordinated (Unc) non-Dpy progeny from *n1855 let-60(gf)/unc-17 dpy-13*, 0/13

segregated *n1855*. From *n1855 let-60(gf)/dpy-9 ced-2 unc-33* hermaphrodites, we isolated Dpy non-Unc progeny, identified hermaphrodites homozygous for the recombinant chromosome, and scored the Ced phenotype. Of Dpy non-Unc recombinants, 3/19 were *ced-2(+) n1855*, 2/19 were *ced-2(−) n1855*, and 14/19 were *ced-2(−) lin-1(+)*. These data position *n1855* left of *unc-17* and between *ced-2* and *unc-33*, an approximately 14-map-unit interval that contains the *lin-1* gene.

Genetic mapping and complementation experiments were used to analyze the recessive abnormal vulva phenotype caused by *n1790*, *n1761*, and *ky54*. *n1761* failed to complement *n1790* and *ky54* for this phenotype, suggesting these three mutations represent one complementation group (data not shown). Three-factor crosses were used to position *n1790* and *n1761* left of *unc-17* on chromosome *IV*, an interval that contains *lin-1*. From *n1790/unc-17 dpy-13* hermaphrodites, 0/9 Unc non-Dpy progeny segregated *n1790* and 8/8 Dpy non-Unc progeny segregated *n1790*. From *n1761/unc-17 dpy-13* hermaphrodites, 0/15 Unc non-Dpy segregated *n1761* and 10/10 Dpy non-Unc progeny segregated *n1761*. To directly test whether these mutations mapped to the *lin-1* locus, we placed *n1761* in *trans* to the loss-of-function allele *lin-1(e1777)*, and screened for recombination between the two mutations. We found zero wild-type recombinants among 1170 self-progeny of *lin-1(e1777)/n1761 dpy-13* hermaphrodites. These data suggest that *n1761* is separated from *lin-1* by less than 0.04 map units and support the hypothesis that *n1761* is an allele of *lin-1*.

Determination of DNA sequences of *lin-1* alleles: For each of the six *lin-1* alleles, genomic DNA was derived from homozygous mutant adult hermaphrodites and was amplified by polymerase chain reaction (PCR) according to Williams *et al.* (1992). *lin-1* contains six exons (Beitel *et al.* 1995). The oligonucleotide primers GBO25f (5′-CCAGCTCGTCACTCATTGC) and GBO26r (5′-GAGCAGATTTGCTTTTAGTAGC) were used to amplify a 322-base pair (bp) DNA fragment containing 64 bp upstream of exon 1, exon 1, intron 1, exon 2, and 63 bp of intron 2. GBO7f (5′-CCTAAAATACCATTAAACTCTC) and GBO14r (5′-CGAGATATAAGCCGTACTACC) amplified a 436-bp fragment containing 77 bp of intron 2, exon 3 and 69 bp of intron 3. GBO16f (5′-TAACCGAAATATGACAAGC) and GBO17r (5′-CCGTCCCTTCAAAATTATTGA) amplified a 490-bp fragment containing 72 bp of intron 3, exon 4 and 137 bp of intron 4. GBO28f (5′-CCTTGCCAAAGATTAGCCG) and GBO20r (5′-GTCTCGACACGAAAAAAGCGGG) amplified a 683-bp fragment containing 119 bp of intron 4, exon 5 and 110 bp of intron 5. GBO21f (5′-GAATTTTCAACAATTTTCA CCC) and GBO27r (5′-AGAAGACTATCGAAAACCCATGGC) amplified a 410-bp fragment containing 105 bp of intron 5 and 305 bp of exon 6 extending 116 bp beyond the stop codon. We purified PCR-amplified DNA fragments and determined the complete sequences of both strands using an automated ABI 373A DNA sequencer (Applied Biosystems, Foster City, CA).

Protein analysis: To produce LIN-1 protein fused to glutathione-S-transferase (GST) or maltose-binding protein (MAL), we cloned fragments of a *lin-1* cDNA (Beitel *et al.* 1995) into pGEX-2T (Pharmacia LKB Biotechnologies, Piscataway, NJ) or pMALP2 (New England Biolabs, Beverly, MA), respectively, using standard techniques (Sambrook *et al.* 1989). The plasmid pDJ29 encodes GST:LIN-1(1–441), pDG14 encodes GST:LIN-1(1–379), pAT4 encodes GST:LIN-1(1–278), pAT2 encodes GST:LIN-1(281–441), pGB35 encodes GST:LIN-1(154–294), and pGB34 encodes MAL:LIN-1(154–294). We used standard *in vitro* mutagenesis techniques to generate pDG29, which encodes GST:LIN-1(1–441P384L). We produced and partially purified fusion proteins using glutathione-sepharose (Pharmacia), essentially according to the manufacturer's instructions. In brief, we transfected plasmids into *Escherichia coli* strain BL21, induced expression with isopropyl thiogalactoside, and made protein extracts using sonication to disrupt cells. Proteins were either soluble in phosphate buffered saline (PBS), or they were solubilized in 7 m urea and then dialyzed against PBS. GST fusion proteins were bound to glutathione-sepharose, eluted using glutathione, glycine, or triethylamine, and dialyzed against MAP kinase assay buffer. To estimate the amount of intact fusion protein in a partially purified sample, we fractionated protein samples by SDS-PAGE, stained the proteins with Coomassie blue, and compared the intensity of the intact fusion protein band to the intensity of known amounts of bovine serum albumin in adjacent lanes. Purified, recombinant, murine Erk2 (New England Biolabs) was assayed as described by Alessi *et al.* (1995). A standard 50-μl reaction was incubated 15 min at 30° and contained 100 μm [^{32}P]ATP (0.15 Ci/mmol) and 0.05 pmol Erk2. To quantify phosphorylation, we measured radioactive protein bound to a P81 filter using a scintillation counter. Purified myelin basic protein was from GIBCO BRL (Gaithersburg, MD).

Anti-LIN-1 antisera were generated by immunizing rabbits with 1 mg of MAL:LIN-1 (154-294) protein in Freund's complete adjuvant (Sigma, St. Louis). After 4, 8, and 12 wk, rabbits were immunized with 1 mg of GST:LIN-1(154-294) in Freund's incomplete adjuvant (Sigma). Sera were collected 2 weeks after each immunization. Western blots were generated as described by Traub *et al.* (1993) and visualized using chemiluminescence.

RESULTS

Isolation and molecular characterization of six novel *lin-1* mutations: We isolated six *lin-1* alleles that are unlike previously described *lin-1(lf)* alleles by performing genetic screens for mutations that prevented Pn.p cells from adopting vulval cell fates (see materials and methods). The alleles *n1855*, *n2515*, and *n2525* were isolated in screens for mutations that suppressed the Muv phenotype caused by a gain-of-function (gf) mutation that constitutively activates the *let-60 ras* gene. The alleles *n1761* and *n1790* were isolated in a screen for mutations that suppressed the Muv phenotype caused by a *lin-15(lf)* mutation. *lin-15* is a negative regulator of vulval cell fates and appears to act upstream of or parallel to *let-60 ras* (reviewed by Kornfeld 1997). The allele *ky54* was recovered as a mutant with a defective vulva in a genetic screen for mutants with an unrelated phenotype.

Complementation tests between these alleles, which caused recessive or semidominant phenotypes, and genetic mapping together suggested that these mutations define a single locus located within an interval on the left arm of chromosome *IV* that contains *lin-1* (see materials and methods). Complementation tests with a *lin-1(lf)* mutation could not be used to test the hypothesis that these mutations affect the *lin-1* gene, because the new mutations did not cause the same abnormalities as a *lin-1(lf)* mutation. Therefore, we investigated whether these were *lin-1* alleles by determining the DNA sequence of the entire *lin-1* coding region and the regions of introns close to the splice sites; we discovered a base

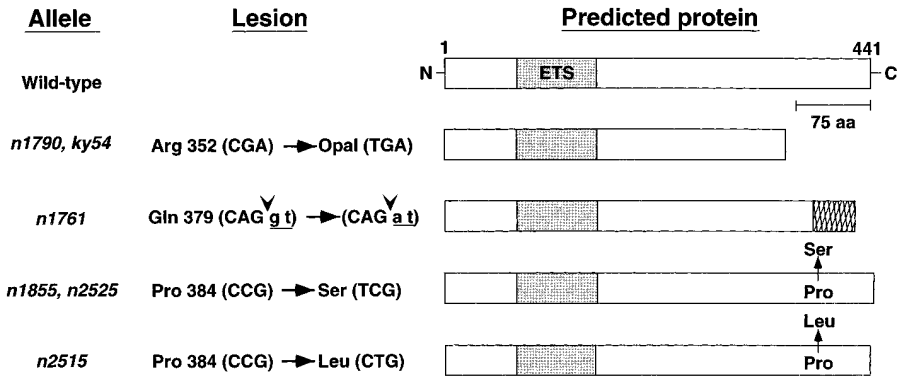

Figure 1.—Base changes in *lin-1(gf)* alleles and predicted mutant proteins. The wild-type amino acid, codon number, and DNA sequence are followed by the corresponding information for the mutant alleles. Opal is a termination codon. An arrowhead indicates the boundary between exon 4, which ends with codon 379, and intron 5, shown underlined and lower case. Each base change was a GC-to-AT transition, the characteristic mutation caused by ethyl methanesulfonate, the mutagen used to generate all of these mutations (Coulondre and Miller 1977). The predicted LIN-1 proteins are drawn to scale, and the ETS domain is stippled. *n1761* mRNA is likely to be spliced abnormally; if intron 5 is not removed, then 45 amino acids encoded by intron 5 will follow residue 379 (hatching). Alternatively, a GT sequence located five bases upstream or five bases downstream of the mutation might function as a cryptic splice site resulting in 64 amino acids encoded by an alternate reading frame of exon 6 following residue 377 or 379, respectively (hatching). We have not directly analyzed the *lin-1* mRNA in *n1761* mutants. *n1855* also contained a C-to-T mutation in intron 5, 21 bp upstream of exon 6; this mutation is probably silent.

change in each of these six strains (Figure 1). The *n1790* and *ky54* alleles contained the same base change, a nonsense mutation at codon 352; the mutant LIN-1 protein is predicted to lack the C-terminal 90 amino acids. The *n1761* allele contained a mutation in the splice site at the 5′ end of intron 5, following codon 379. Intron 5 is likely to be retained or removed by the use of a cryptic splice site; in either case about 62 amino acids at the C terminus would be replaced by about 50 new amino acids (see Figure 1 legend). The *n1855* and *n2525* alleles contained the same base change, a missense mutation that changes amino acid 384 from proline to serine. The *n2515* allele also contained a base change in codon 384; this mutation changes proline to leucine (Figure 1). Thus, these six independently derived mutations represent four different molecular changes. All four affect the predicted C terminus of LIN-1.

The novel *lin-1* mutations caused larval lethality: To investigate the abnormalities caused by these *lin-1* mutations, we observed the development of mutant animals using a dissecting microscope. These mutations caused larval lethality that varied in penetrance from 73% for *n1761* to 5% or less for *n2515*, *n2525*, and *n1855* (Table 1). Most affected animals died during the first or second larval stage and were thin and straight. This phenotype of rigid, rod-like larval lethality appeared to be identical to that caused by loss-of-function mutations in many genes involved in vulval induction: *lin-3*, *let-23*, *sem-5*, *let-60 ras*, *lin-45 raf*, *ksr-1*, *mek-2*, and *mpk-1* (Ferguson and Horvitz 1985; Han *et al.* 1990, 1993; Clark *et al.* 1992; Wu and Han 1994; Kornfeld *et al.* 1995a,b; Sundaram and Han 1995). In *let-60(lf)* mutants, this lethality results from a failure to establish the excretory duct cell fate (Yochem *et al.* 1997).

A *lin-1* loss-of-function mutation does not cause larval lethality and can suppress the larval lethality caused by a loss-of-function mutation in these signaling genes (Han *et al.* 1990; Kornfeld *et al.* 1995a,b; Sundaram and Han 1995). These observations suggest that *lin-1* activity causes larval lethality and the RTK-Ras-MAP kinase signaling pathway promotes viability by negatively regulating *lin-1*. The finding that these novel *lin-1* alleles caused larval lethality suggests that these are gain-of-function alleles that produce constitutively active protein that cannot be negatively regulated.

Loss-of-function mutations in *let-60 ras*, *mek-2*, and *mpk-1* cause hermaphrodite sterility characterized by germ cells that cannot exit from pachytene (Church *et al.* 1995). These six *lin-1* mutations did not cause significant hermaphrodite sterility (data not shown), suggesting that *lin-1* is not involved in germ cell maturation.

The novel *lin-1* mutations caused vulval defects: These new *lin-1* mutants displayed protruding vulval tissue and defects in egg laying, possible indications of abnormalities in the vulval passageway. The penetrance of these defects varied from more than 50% for *n1790* and *ky54* to 6% or less for *n2515*, *n2525*, and *n1855* (Table 1). To determine whether these *lin-1* mutations caused defects in vulval cell fates, we used Nomarski optics to examine the cells that form the vulva in fourth larval stage (L4) animals. The cell lineage of *C. elegans* is nearly invariant, and wild-type hermaphrodites have 22 descendants of P5.p, P6.p, and P7.p (Sulston and Horvitz 1977). By contrast, *n1790* and *n1761* hermaphrodites had an average of 20 descendants of these cells and sometimes had as few as 17 descendants (Table 1). Furthermore, these mutants often had grossly abnormal vulval invaginations and large Pn.p descendants that appeared to have undergone too few cell divisions. We never observed these abnormalities in wild-type animals. These abnormalities are similar to the defects in vulval formation caused by partial loss-of-function mutations

TABLE 1

Phenotypes of *lin-1* mutants

Genotype	Percentage dead larvae	Percentage abnormal vulva	n^a	P5.p–P7.p descendants	n^b
Wild type	0	0	200	22 (22)	10
n1761	73	31	359	20 (17–22)	10
n1790	17	54	285	20 (17–24)	10
ky54	49	59	143	ND[c]	
n2515[d]	5	3	167	22 (22)	9
n2525[d]	1	3	184	22 (21–22)	10
n1855[d]	2	6	185	ND	
smg-1; n1790[e]	43	81	168	15 (10–22)	11

For percent dead larvae and abnormal vulva, we placed each egg on a separate Petri dish and observed development at 20°. Percent dead larvae, the percent of all hatched eggs that generated dead larvae; most dead larvae displayed a rigid, rod-like morphology. Percent abnormal vulva, the percent of all adult hermaphrodites that displayed a severe egg-laying defect or a protruding vulva. P5.p–P7.p descendants, the number of nuclei that appeared to be descendants of P5.p, P6.p, and P7.p based on appearance and position in L4 hermaphrodites at the "Christmas tree" stage of vulval development. The number is an average followed by the smallest and largest values observed. Differences between the phenotypes of the *n1790* strain and the *ky54* strain were probably caused by genetic differences at sites other than the *lin-1* locus, presumably as a result of prior mutagenesis.

[a] *n*, number of hatched eggs analyzed.

[b] *n*, number of L4 hermaphrodites examined.

[c] ND, not determined.

[d] These strains also contained *dpy-13*. *dpy-13* mutants did not display significant larval lethality or abnormal vulvae (data not shown).

[e] This strain also contained *unc-54(r293)*; the Unc phenotype is suppressed by *smg-1* (Pulak and Anderson 1993).

in signaling genes, such as *lin-45 raf* (Han *et al.* 1993), and are less severe than the defects in vulval formation caused by strong loss-of-function mutations in signaling genes. For example, a null allele of *mek-2* causes P5.p, P6.p, and P7.p to adopt the 3° fate and generate a total of six descendants that form no vulval invagination (Kornfeld *et al.* 1995a). We interpret the defects in *n1790* and *n1761* mutants as a weak Vul phenotype that results from vulval cell lineage defects. The vulval invaginations of *n2515* and *n2525* animals appeared normal and had an average of 22 descendants of P5.p, P6.p, and P7.p (Table 1). Thus, we observed a correlation between the number of descendants of P5.p, P6.p, and P7.p and the severity of the abnormal vulva phenotype, suggesting that these cell-fate defects caused the gross vulval abnormalities.

To characterize further the effect of these *lin-1* alleles on vulval development, we examined double mutants containing *let-60 ras* or *lin-15* mutations that cause a Muv phenotype. The *lin-1* alleles partially suppressed the *lin-15(lf)* Muv phenotype and partially or completely suppressed the *let-60(gf)* Muv phenotype (Table 2). These alleles can be ordered on the basis of their ability to suppress these two Muv phenotypes: *n2515* and *n2525* were the most effective, followed by *n1761* and *n1790*. To investigate the cellular basis for the suppression of the *let-60(gf)* Muv phenotype, we examined the descendants of the Pn.p cells in L4 animals. Whereas in *let-60(gf)* animals, 53% of the cells P3.p, P4.p, and P8.p adopted vulval fates ($n = 10$ animals), in *lin-1(n2515) let-60(gf)* animals, 0% of the cells P3.p, P4.p, and P8.p adopted vulval fates ($n = 10$ animals; Figure 2, A and B). Thus, the *lin-1(n2515)* mutation prevented P3.p, P4.p, and P8.p from adopting vulval fates in response to mutationally activated LET-60 Ras, but *n2515* did not prevent P6.p from adopting a vulval fate in response to the anchor cell signal. Our interpretation of these findings is that *n2515* partially suppresses Ras-mediated signaling; the anchor cell signal overcomes the *n2515* suppression by strongly activating *let-60 ras* in P6.p, whereas the *let-60(gf)* mutation does not overcome the *n2515* suppression since it only partially activates *let-60 ras* in P3.p, P4.p, and P8.p. The anchor cell signal may also activate pathways that function in parallel to *let-60 ras*, and factors other than the anchor cell signal may cause P6.p to be more likely to adopt a vulval fate than P3.p, P4.p, and P8.p.

A *lin-1(lf)* mutation causes a Muv phenotype that is epistatic to the Vul phenotype caused by loss-of-function mutations in genes in the RTK-Ras-MAP kinase signaling pathway (Ferguson *et al.* 1987). These observations suggest that *lin-1* activity causes Pn.p cells to adopt the nonvulval 3° fate and that the RTK-Ras-MAP kinase signaling pathway promotes the 1° vulval cell fate by regulating *lin-1* negatively. The finding that these new *lin-1* alleles caused Pn.p cells to adopt nonvulval fates sug-

TABLE 2

***lin-1* double mutants**

Genotype	Percentage Muv	*n*[a]
Wild type	0	200
let-60(gf)[b]	64	637
n2515 let-60(gf)	0	515
n2525 let-60(gf)	0	516
n1855 let-60(gf)	1	547
n1761 let-60(gf)	8	527
n1790 let-60(gf)	44	449
lin-15(lf)[c]	100	624
n2515; lin-15(lf)[d]	51	574
n2525; lin-15(lf)[d]	58	373
n1761; lin-15(lf)	70	504
n1790; lin-15(lf)	78	550
lin-31(lf)[e]	64	490
n2515; lin-31(lf)[d]	71	577
n2525; lin-31(lf)[d]	75	507
n1761; lin-31(lf)	83	207
n1790; lin-31(lf)	98	428

We scored all the adult hermaphrodites on several Petri dishes for the Muv phenotype, one or more ventral protrusions displaced from the position of the vulva.

[a] *n*, number of hermaphrodites examined.

[b] *let-60(n1046gf).*

[c] *lin-15(n765ts).*

[d] These strains also contained *dpy-13*.

[e] *lin-31(n1053).*

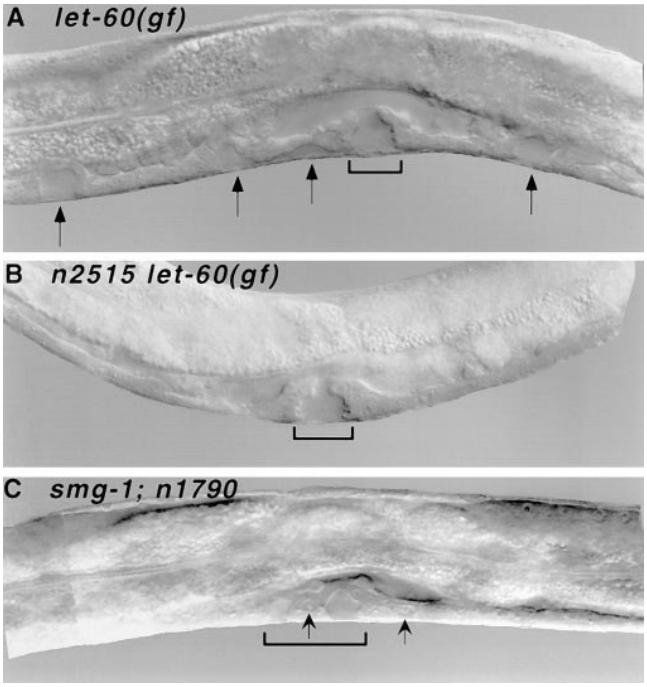

Figure 2.—*lin-1(gf)* mutations prevent Pn.p cells from adopting vulval fates. Photomicrographs of Nomarski images of L4 hermaphrodites at the "Christmas tree" stage of vulval development. In these lateral views, anterior is left and ventral is down. (A) *let-60(n1046gf)* mutant with a normal vulval invagination (bracket) and four ectopic invaginations (arrows) that resulted from the adoption of vulval fates by P3.p, P4.p, and P8.p. (B) *lin-1(n2515) let-60(n1046gf)* mutant with a normal vulval invagination (bracket) and no ectopic invaginations, because P3.p, P4.p, and P8.p adopted the nonvulval 3° fate. (C) *smg-1; lin-1(n1790)* mutant with an abnormal vulval invagination (bracket), which was divided into two small, irregularly shaped invaginations and contained only 13 Pn.p descendants. These included two large descendants that probably did not undergo the normal number of divisions (arrows). *n1790* single mutants displayed similar but less severe defects.

gests that they are gain-of-function alleles that produce constitutively active protein that cannot be negatively regulated.

Two observations suggest that at least some of these *lin-1* alleles do more than simply increase *lin-1* activity. First, although many *n1790* and *n1761* mutants displayed a weak Vul phenotype, we occasionally observed a mutant animal that displayed a Muv phenotype, suggesting those mutant animals had a reduced amount of *lin-1* activity. Second, a comparison of the penetrance of the larval-lethal, abnormal-vulva, and suppression-of-Muv phenotypes shows that these *lin-1* alleles cannot be arranged in a simple allelic series. For example, *n1761* caused the highest penetrance of larval lethality but only partially suppressed the *let-60(gf)* Muv phenotype (Tables 1 and 2). By contrast, *n2515* and *n2525* caused the lowest penetrance of larval lethality but completely suppressed the *let-60(gf)* Muv phenotype. As described in the discussion, these observations suggest that these alleles affect more than one aspect of *lin-1* function.

The novel *lin-1* mutations cause gain-of-function phenotypes and result in altered gene activity: To understand how these mutations affect the activity of the *lin-1* gene, we compared these *lin-1* alleles to *lin-1(sy254)*, a null mutation by genetic criteria and by molecular criteria, since exons 3 and 6 are deleted and exons 4 and 5 are rearranged (Beitel *et al.* 1995). We also analyzed the effects of varying *lin-1* gene dosage using *mDp1*, a free duplication that contains *lin-1* and genes positioned right and left of *lin-1* (Rogalski and Riddle 1988). By comparing *n1761/n1761* animals (73% lethal, 31% abnormal vulva) with *n1761/null* animals (10% lethal, 10% abnormal vulva), we conclude that larval lethality and abnormal vulva formation are gain-of-function phenotypes, since their penetrance was reduced in *trans* to a *lin-1(null)* mutation (Table 3). Similarly, *n1790/n1790* animals (17% lethal, 54% abnormal vulva) displayed a higher penetrance of these defects than *n1790/null* animals (0% lethal, 12% abnormal vulva). These findings also show that the gain-of-function phenotypes caused by *n1761* and *n1790* are dosage sensitive, since two mutant alleles caused more severe defects than one mutant allele. By contrast, the Muv phenotype caused by *n1790* was more severe in *n1790/null* animals (75%) than in *n1790/n1790* animals (11%) (Table 3). Thus, the Muv phenotype appears to be a loss-of-function phenotype, which is consistent with previous analyses of *lin-1* (Beitel *et al.* 1995). The finding that the *n1790*

TABLE 3

Dosage studies with *n1761* and *n1790*

Genotype	Percentage dead larvae	Percentage abnormal vulva	Percentage Muv	*n*
+/+	0	0	0	200
n1761/null[a]	10	10	1	490
n1761/+[b]	0	0	0	553
n1761/n1761	73	31	9	359
n1761/n1761/+[c]	ND[d]	16	0	183
smg-1; n1761/n1761[e]	64	28	8	181
n1790/null[f]	0	12	75	139
n1790/+[g]	0	0	0	67
n1790/n1790	17	54	11	285
n1790/n1790/+[h]	ND[d]	13	1	163
smg-1; n1790/n1790[e]	43	81	12	168
smg-1[e]	ND	0	0	303

For homozygous strains, we placed each egg on a separate Petri dish and observed development. Heterozygous animals were generated in mating experiments using marker mutations to distinguish self-progeny from cross-progeny. Columns are as defined in Tables 1 and 2.

[a] These *n1761/lin-1(sy254) unc-24* hermaphrodites were non-uncoordinated (non-Unc) cross-progeny of *n1761* males and *lin-1(sy254) unc-24/nT1 n754* hermaphrodites. The *nT1 n754* chromosome causes a recessive lethal and dominant Unc phenotype.

[b] These hermaphrodites were Unc non-Dpy cross-progeny of wild-type males and *n1761; dpy-11 unc-41* hermaphrodites.

[c] These *n1761 dpy-13; mDp1* hermaphrodites were non-Dpy self-progeny of hermaphrodites with the same genotype. *mDp1* contains *lin-1*(+) and *dpy-13*(+).

[d] ND, not determined. We could not reliably determine the percent dead larvae of animals of this genotype, because *mDp1* is not transmitted to every progeny animal, and *mDp1* rescue of the Dpy-13 phenotype cannot be scored in dead larvae.

[e] These strains also contained *unc-54(r293).*

[f] These animals were genotype *n1790/lin-1(sy254) unc-24*; we picked non-Unc cross-progeny of *n1790/+* males and *lin-1(sy254) unc-24/nT1 n754* hermaphrodites, scored their phenotype, and confirmed their genotype by examining self-progeny.

[g] These hermaphrodites were Unc non-Dpy cross-progeny of wild-type males and *n1790; dpy-11 unc-41* hermaphrodites.

[h] These *n1790 dpy-13; mDp1* hermaphrodites were non-Dpy self-progeny of hermaphrodites of the same genotype.

mutation caused both a gain and loss of gene activity suggests this mutation affects more than one aspect of *lin-1* gene function.

The larval lethality and vulval abnormalities caused by *n1761* and *n1790* were reduced by *lin-1*(+) (Table 3, compare *n1761/null* with *n1761/+*, *n1761/n1761* with *n1761/n1761/+*, *n1790/null* with *n1790/+*, and *n1790/n1790* with *n1790/n1790/+*). If these defects resulted from an increase in the amount of wild-type *lin-1* activity, then an additional copy of *lin-1*(+) should have enhanced the severity of these defects. The finding that *lin-1*(+) reduced the severity of these defects suggests that these mutations result in an altered *lin-1* activity that can be suppressed by *lin-1*(+). These findings are consistent with the model that these mutant *lin-1* alleles cannot be negatively regulated and thus are active in cells in which *lin-1*(+) is normally inactivated. Although *lin-1*(+) is functionally inactive in such cells, it might still compete with mutant *lin-1* for limiting cofactors.

To analyze *n2515* and *n2525*, we measured the suppression of the *let-60(gf)* Muv phenotype. The *let-60(gf)* mutation caused 64% of the animals to be Muv (Table 4). In *trans* to a wild-type *lin-1* allele, *n2515* and *n2525* reduced the penetrance of this Muv phenotype to 3% (*n2515/+*) and 15% (*n2525/+*) (Table 4). By contrast, a heterozygous *lin-1(null)* allele enhanced the *let-60(gf)* Muv phenotype to 98% (*null/+*) (Table 4). Thus, the suppression of *let-60(gf)* Muv is a gain-of-function phenotype. *n2515/n2515* and *n2515/null* animals both displayed strong suppression of the *let-60(gf)* Muv phenotype, suggesting the *n2515* suppression of *let-60(gf)* Muv phenotype is not dosage sensitive (Table 4, lines 4 and 5). *n2525* caused a phenotype that was slightly dosage sensitive—whereas two mutant copies (*n2525/n2525*) reduced the *let-60(gf)* Muv phenotype to 0%, one mutant copy reduced the penetrance to 12% (*n2525/null*) (Table 4). The suppression of *let-60(gf)* Muv by *n2515* and *n2525* resulted from an altered *lin-1* activity rather than from a simple increase of *lin-1* activity, since the phenotype was not enhanced but rather was reduced somewhat by an extra copy of wild-type

TABLE 4

Dosage studies with *n2515* and *n2525*

Genotype	Percentage Muv	*n*
let-60(gf)	64	637
null/+ let-60(gf)[a]	98	315
n2515/+ let-60(gf)[b]	3	360
n2515/n2515 let-60(gf)	0	515
n2515/null let-60(gf)[c]	1	392
n2515/n2515/+ let-60(gf)[d]	22	296
n2525/+ let-60(gf)[e]	15	287
n2525/n2525 let-60(gf)	0	516
n2525/null let-60(gf)[f]	12	509
n2525/n2525/+ let-60(gf)[g]	41	340

For homozygous strains, we scored all adult hermaphrodites on several Petri dishes for the Muv phenotype. Heterozygous animals were either cross-progeny from mating experiments, in which case marker mutations were used to distinguish self-progeny from cross-progeny, or they were self-progeny of heterozygous animals, in which case marker mutations were used to distinguish homozygous from heterozygous progeny. Columns are as defined in Table 2.

[a] These *lin-1(sy254) let-60(gf) dpy-20/unc-17 dpy-13 let-60(gf)* hermaphrodites were non-Dpy self-progeny of hermaphrodites of the same genotype.

[b] These hermaphrodites were non-Dpy cross-progeny of *n2515 let-60(gf)* males and *let-60(gf) dpy-20* hermaphrodites.

[c] These *lin-1(sy254) let-60(gf) dpy-20/n2515 dpy-13 let-60(gf)* hermaphrodites were non-Dpy self-progeny of hermaphrodites of the same genotype.

[d] These *n2515 dpy-13 let-60(gf); mDp1* hermaphrodites were non-Dpy self-progeny of hermaphrodites of the same genotype.

[e] These hermaphrodites were non-Dpy cross-progeny of *n2525 let-60(gf)* males and *let-60(gf) dpy-20* hermaphrodites.

[f] These *lin-1(sy254) let-60(gf) dpy-20/n2525 dpy-13 let-60(gf)* hermaphrodites were non-Dpy self-progeny of hermaphrodites of the same genotype.

[g] These *n2525 dpy-13 let-60(gf); mDp1* hermaphrodites were non-Dpy self-progeny of hermaphrodites of the same genotype.

lin-1 (Table 4, compare line 4 to 6 and line 8 to 10). The effect of *mDp1* was greater than the effect of *lin-1*(+) contained on an intact chromosome *IV*; this effect may result from genes other than *lin-1* present on *mDp1*.

A *smg* mutation enhanced the *lin-1(n1790)* gain-of-function phenotype: *C. elegans* contains a surveillance system that degrades transcripts that contain a premature stop codon (Pulak and Anderson 1993). Therefore, a nonsense mutation results in both a truncated protein and the production of less protein than normal because the mutant mRNA is relatively unstable. It is possible to eliminate the second effect of a nonsense mutation by creating a double mutant with a *smg* mutation; the *smg* genes are required for the function of the surveillance system, and mRNAs with premature stop codons accumulate to essentially wild-type levels in *smg*(−) mutants (Pulak and Anderson 1993).

Of the four different *lin-1(gf)* mutations, only *n1790* is a nonsense change. Our results indicated that the larval lethality and abnormal vulva caused by *n1790* are dose-dependent, gain-of-function phenotypes. If this model is correct, then we predict that stabilizing the mutant *lin-1(n1790)* mRNA and producing more LIN-1(Arg352stop) protein would enhance these phenotypes. Table 1 shows that *smg-1; lin-1(n1790)* double mutants displayed significantly more larval lethality (43% versus 17%) and abnormal vulvae (81% versus 54%) than did *n1790* single mutants. To investigate the cause of the vulval defects, we determined the number of P5.p, P6.p, and P7.p descendants in the vulval invaginations of L4 hermaphrodites. *smg-1; n1790* animals had an average of 15 descendants, compared to an average of 20 descendants for *n1790* mutants and 22 descendants for wild-type animals (Table 1 and Figure 2C). Thus, the *smg-1* mutation enhanced the *n1790* Vul phenotype. In control experiments, the *smg-1* mutation alone did not cause significant vulval defects, and it did not enhance the defects caused by *n1761*, a mutation in a splice site (Table 3, lines 4, 6, and 12). These observations support the model that LIN-1(Arg352stop) protein encoded by *n1790* prevents P6.p from adopting a vulval fate and causes larval lethality in a dose-dependent manner. Furthermore, *lin-1(n1790)* mRNA appears to be less stable than *lin-1*(+) mRNA, suggesting the loss-of-function Muv phenotype caused by *n1790* may be a consequence, at least in part, of reduced protein levels caused by mRNA instability.

***lin-1* acts parallel to or upstream of *lin-31*:** A *lin-31(lf)* mutation causes a partially penetrant Muv phenotype, suggesting *lin-31* activity prevents P3.p, P4.p, and P8.p from adopting vulval fates (Ferguson *et al.* 1987). The predicted LIN-31 protein contains an HNF-3/*forkhead* DNA-binding domain and presumably functions as a transcription factor (Miller *et al.* 1993). Genetic epistasis experiments suggest *lin-31* functions downstream of *mpk-1* ERK MAP kinase, if these genes act in a linear pathway (Lackner *et al.* 1994). Previously, it had not been possible to use genetic epistasis experiments to investigate the order of action of *lin-31* and *lin-1*, because a loss-of-function mutation in either gene causes a Muv phenotype. We used the *lin-1(gf)* mutations, which suppressed the Muv phenotype caused by *let-60(gf)* and *lin-15(lf)* mutations, to explore the relationship between *lin-1* and *lin-31*. Table 2 shows that none of the *lin-1(gf)* mutations suppressed the *lin-31* Muv phenotype. These results suggest that if *lin-1* and *lin-31* act in a linear pathway, *lin-1* acts upstream of *lin-31*. These data are also consistent with the possibility that *lin-1* and *lin-31* function in parallel. We favor this possibility, since both genes encode predicted transcription factors.

It is noteworthy that all the *lin-1(gf); lin-31(lf)* double mutant strains displayed a higher penetrance Muv phenotype than the *lin-31(lf)* single mutant strain (Table 2). We interpret these results as an indication that these *lin-1* mutations partially reduce *lin-1* activity, resulting in

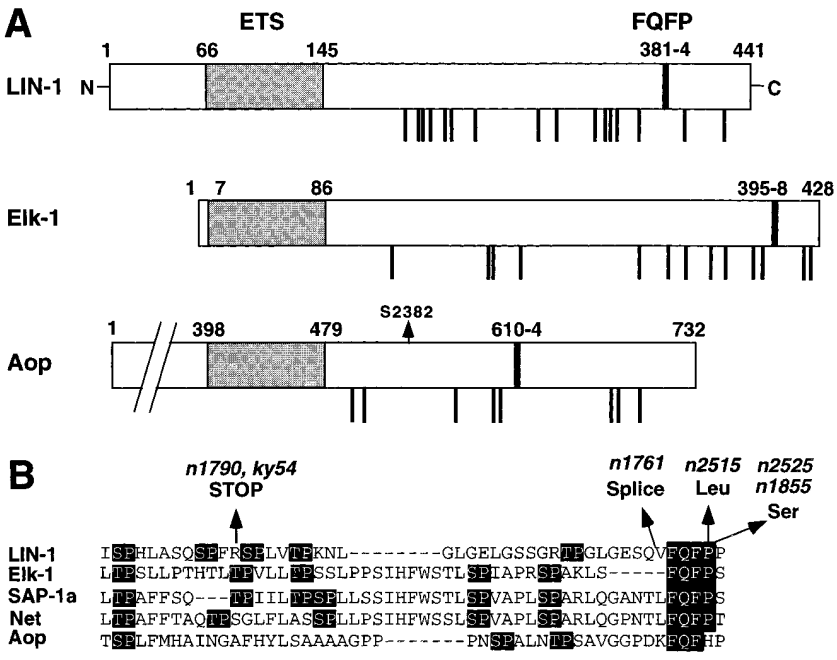

Figure 3.—LIN-1 and Aop contain a C box. (A) In the diagrams of *C. elegans* LIN-1 (Beitel *et al.* 1995), human Elk-1 (Rao *et al.* 1989), and Drosophila Aop (Lai and Rubin 1992), the 80-amino-acid ETS domain is stippled, the FQFP motif is black, and S/TP sequences (potential MAP kinase phosphorylation sites) C-terminal to the ETS domain are indicated by vertical lines shown below. The first and last residue in a motif and the first and last residue in each protein are numbered. The N terminus of Aop is not drawn to scale. The *aop*^{yanS2382} mutation (arrow) is a 5 base pair deletion that shifts the reading frame, thereby replacing the C-terminal 162 amino acids with a new group of 86 amino acids (Rebay and Rubin 1995). (B) The C boxes of human Elk-1 (residues 352–399; Rao *et al.* 1989), human SAP-1a (residues 353–402; Dalton and Treisman 1992) and murine Net (residues 328–380; Giovane *et al.* 1994) are aligned with the corresponding regions of LIN-1 (residues 341–385; Beitel *et al.* 1995) and Aop (residues 569–614; Lai and Rubin 1992). The FQFP and S/TP sequences are shaded. The positions and types of defect caused by *lin-1(gf)* mutations are shown above.

a weak *lin-1(lf)* Muv phenotype. The *lin-31(lf)* mutation appears to create a sensitive background that can be used to measure this effect. The alleles *n2515* and *n2525*, which encode proteins with a single amino acid change, increased the penetrance of the Muv phenotype only slightly, suggesting that these mutations result in only a slight reduction of *lin-1* activity. The alleles *n1790* and *n1761*, which encode truncated proteins, increased the penetrance of the Muv phenotype moderately, suggesting that these mutations result in a more significant reduction of *lin-1* activity.

***lin-1(gf)* mutations affect a conserved motif in the C box:** The vertebrate proteins Elk-1, SAP-1a, and Net/ERP/SAP-2 are classified as members of the Elk subfamily of ETS proteins because they share three regions of significant sequence conservation: an N-terminal ETS domain, a centrally positioned B box, and a C-terminal C box (reviewed by Wasylyk *et al.* 1993; Giovane *et al.* 1994; Treisman 1994). Based on the positions and sequences of their ETS domains and the positions and sequences of regions similar to the C box, we propose that LIN-1 and Drosophila Aop are members of the Elk subfamily. The ETS domain of LIN-1 shares more sequence identity with the ETS domain of human Elk-1 (67% identity) and human SAP-1a (61% identity) than with any other ETS domain (Beitel *et al.* 1995). Likewise, the ETS domain of Aop is most similar to the ETS domain of Elk-1 (51% identity; Lai and Rubin 1992). The ETS domains of LIN-1 and Aop are somewhat less similar (41% identity; Beitel *et al.* 1995). LIN-1 (441 residues), Elk-1 (428 residues), SAP-1a (453 residues) and Net (409 residues) are similarly sized and have ETS domains similarly positioned in the N-terminal region (Figure 3A). By comparison, Aop (688 residues) is larger and has more residues N-terminal to the ETS domain, which is located near the center of the protein. However, the number of residues C-terminal to the ETS domain is similar in Aop and the other four proteins (Figure 3A).

Further evidence that ETS proteins are members of a subfamily is sequence similarity outside the ETS domain. By studying the C termini of these proteins, we found that LIN-1, Elk-1, SAP-1a, and Net each have the sequence FQFP, while Aop has the sequence FQFHP (Figure 3B). In Elk-1, SAP-1a, and Net, the FQFP sequence is at the end of the C box (Giovane *et al.* 1994; Treisman 1994). The C boxes of ELK-1, SAP-1a, and Net are characterized by five or six S/TP sequences, which are potential MAP kinase phosphorylation sites. In the corresponding regions, LIN-1 has five S/TP sequences and Aop has three (Figure 3B). Elk-1, SAP-1a, and Net have additional identities in the C box that are not conserved in LIN-1 and Aop. These observations suggest that LIN-1 and Aop contain divergent C boxes. Thus, *lin-1*, *aop*, *elk-1*, *sap-1*, and *net* appear to be derived from an ancestral gene that encoded a protein with an N-terminal ETS domain and a C-terminal C box.

All the *lin-1(gf)* mutations result in changes in the FQFP motif. *lin-1(n1790)* and *lin-1(n1761)* encode truncated proteins that lack the FQFP motif. *lin-1(n2525)* and *lin-1(n2515)* result in a change to FQFS or FQFL, respectively (Figure 3B). Our genetic experiments indicate that these mutations impair the negative regulation of *lin-1*, suggesting the conserved FQFP motif may be important for this negative regulation.

LIN-1 is phosphorylated by ERK MAP kinase *in vitro*:

To investigate whether LIN-1 is phosphorylated by ERK MAP kinase, we used the *lin-1* cDNA to express in *E. coli* full-length LIN-1 protein fused to GST. We partially purified this protein by affinity chromatography and assayed its ability to be phosphorylated by purified, recombinant, murine Erk2 MAP kinase. The GST:LIN-1(1–441) fusion protein was a high-affinity substrate for Erk2 with a K_m of 0.18 μm (Figure 4). This K_m is about 18-fold lower than the 3.3 μm K_m of myelin basic protein (MBP), a protein frequently used to assay ERK activity. The relative acceptor ratio (V_{max}/K_m) is an overall measure of the ability of a protein to function as a substrate. The relative acceptor ratio of GST:LIN-1(1–441) was 7-fold higher than the value for MBP (Figure 4).

To investigate the regions of LIN-1 that are important for phosphorylation, we generated and assayed fragments of LIN-1 fused to GST. GST:LIN-1(1–379) includes the residues predicted to be encoded by *lin-1(n1761)*. This protein lacks the C-terminal 62 amino acids and the FQFP motif but contains the S/TP motifs in the C box. GST:LIN-1(1–379) had a K_m of 1.1 μm, which is about 6-fold higher than the K_m of full-length LIN-1, and a V_{max} that was similar to the V_{max} of full-length LIN-1 (Figure 4). The difference in K_m values suggests that the deleted region is important for the high-affinity interaction between LIN-1 and Erk2, while the similarity in V_{max} values suggests that this LIN-1 fragment contains the phosphorylation site(s). GST:LIN-

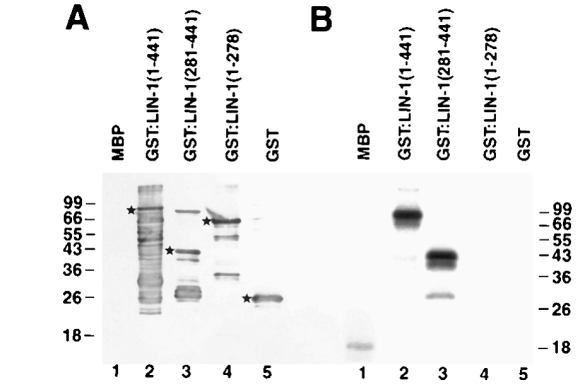

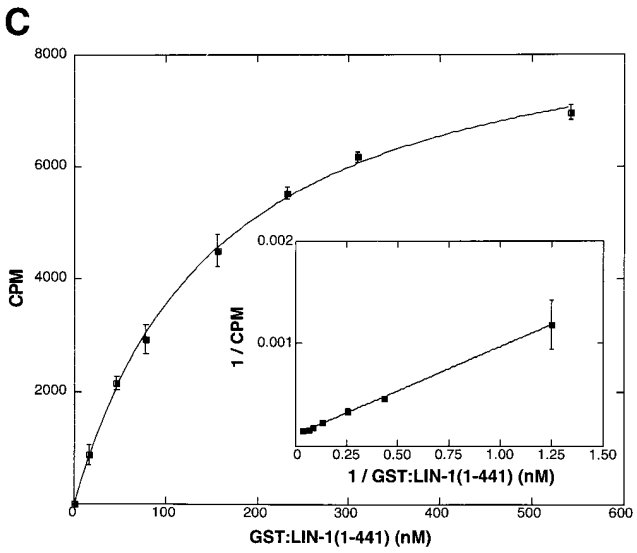

D

Protein	K_m (uM)	V_{max} (pmol PO_4/ min/pmol Erk2)	Relative Acceptor Ratio
MBP	3.3 ± 0.5	63 ± 1	1
GST:LIN-1(1-441)	0.18 ± 0.006	24 ± 7	7
GST:LIN-1(1-441P384L)	0.8 ± 0.2	44 ± 15	3
GST:LIN-1(1-379)	1.1 ± 0.1	36 ± 2	2
GST:LIN-1(1-278)	40 ± 6	8 ± 2	0.01
GST:LIN-1(281-441)	0.76 ± 0.04	40 ± 3	3

Figure 4.—LIN-1 is phosphorylated by ERK MAP kinase. Each protein listed in D was analyzed using the same experimental approaches; A–C show examples of these data. (A) A Western blot of samples containing partially purified GST or GST fused to the indicated LIN-1 residues that were treated with an anti GST:LIN-1(154–294) antiserum. Lines indicate the positions of protein standards from an adjacent lane, with sizes in kilodaltons (kD). This experiment shows that each sample contained intact fusion protein (indicated by a star) that reacted with the antiserum and migrated with the predicted molecular weight [myelin basic protein (MBP), 18 kD; GST:LIN-1(1–441), 74 kD; GST:LIN-1(281–441), 43 kD; GST:LIN-1(1–278), 58 kD; GST, 26 kD]. We adjusted the amount of total protein loaded in each lane to achieve a similar signal intensity of intact protein. Most samples also contained lower molecular weight forms that reacted with the antiserum and are likely to be fragments of fusion proteins that were generated by protease activity in *E. coli*. These samples also contained endogenous bacterial proteins that were visible on Coomassie blue-stained gels (data not shown) and usually did not react with the antiserum. However, the uppermost band in lane 3 did react with this antiserum and appears to be an endogenous bacterial protein, since we observed the same band in partially purified samples of unrelated GST fusion proteins (data not shown). MBP did not react with the antiserum. (B) Equal amounts of intact GST or GST:LIN-1 fusion proteins were incubated with purified, recombinant, murine Erk2 and [^{32}P]ATP, fractionated by SDS-PAGE, and visualized by autoradiography. GST:LIN-1(1–441) and GST:LIN-1(281–441) were strongly labeled, whereas GST alone or GST:LIN-1(1–278) showed no significant incorporation. MBP was weakly labeled. The GST:LIN-1(1–441) sample contained many proteolytic fragments that bound to the affinity column and thus are likely to contain GST and lack portions of the LIN-1 C terminus. Strikingly, only full-length LIN-1 protein was labeled, suggesting most or all of the C terminus is necessary for phosphorylation. (C) A kinetic analysis showing the amount of ^{32}P incorporated measured by filter binding and scintillation counting (counts per minute, CPM) in assays with increasing amounts of GST:LIN-1(1–441). Assays were terminated after 15 min, at which point ^{32}P incorporation was linear with respect to time. Values are the average of two samples, a bar indicates the range. The inset shows a Lineweaver-Burke plot of the data. (D) Kinetic analyses were performed as described above using seven concentrations of intact proteins, usually ranging from 0.2 K_m to 2.0 K_m. K_m and V_{max} were calculated from the intercepts of Lineweaver-Burke plots; in each case the data closely approximated a straight line. Values are the average and one standard deviation of three or four separate experiments. To determine V_{max}, we calculated total phosphate incorporated using the measured CPM and the specific activity of the [^{32}P]ATP, and factored in the assay time (15 min) and the amount of Erk2 used (about 0.03 pmol). Relative acceptor ratio is V_{max}/K_m; values were normalized by assigning a value of 1.0 to MBP.

1(1–278) lacks the C-terminal 163 amino acids and the entire C box. This protein was an extremely poor substrate for Erk2 with a relative acceptor ratio that was 200-fold lower than the value for GST:LIN-1(1–379) (Figure 4D). These findings suggest that the region from amino acid 278 to 379 may contain the normal phosphorylation site(s). GST:LIN-1(281–441) contains the C-terminal 160 amino acids and includes the C box; it had a relative acceptor ratio that was about 300-fold higher than the N-terminal region of LIN-1 (Figure 4D). Thus, the C terminus of LIN-1 was necessary for efficient phosphorylation of LIN-1 and sufficient to function as a substrate for Erk2.

To investigate how the *lin-1(gf)* missense mutations affect phosphorylation by ERK, we generated full-length LIN-1 containing the change encoded by *lin-1(n2515)*. GST:LIN-1(1–441P384L) had a K_m of 0.8 μm, which is about fourfold higher than the K_m of wild-type LIN-1, and a V_{max} similar to that of wild-type LIN-1. Thus, changing FQFP to FQFL reduced the binding affinity of Erk2.

DISCUSSION

***lin-1* activity promotes nonvulval fates and larval lethality:** We identified and characterized six mutations that define a new class of *lin-1* allele. Our genetic analysis suggests that these mutations affect two aspects of *lin-1* function. First, they have a major effect on the ability of *lin-1* to be negatively regulated, which results in constitutively active *lin-1* and causes larval lethality, a vulvaless phenotype, and a suppression of Muv phenotype. These are gain-of-function phenotypes. Our results suggest that negative regulation depends on the ability of LIN-1 protein to be phosphorylated by MAP kinase. Second, these mutations have a minor effect on the ability of *lin-1* to control cell fates, which results in inactive *lin-1* and causes a loss-of-function Muv phenotype. The LIN-1 protein presumably controls cell fates by binding DNA and regulating transcription. The missense mutations *n2515* and *n2525* did not significantly impair the ability of *lin-1* to control cell fates, because they caused only a slight Muv phenotype. These mutations partially impaired the ability of *lin-1* to be negatively regulated, because they caused weak gain-of-function phenotypes (larval lethality and Vul). The proline-to-leucine change caused by *n2515* impaired negative regulation more than the proline-to-serine change caused by *n2525*; although the difference was small, it was observed in multiple genetic backgrounds. The alleles *n1790* and *n1761*, which are predicted to encode truncated proteins, partially impaired the ability of *lin-1* to control cell fates, because they caused a Muv phenotype of low penetrance. These mutations severely impaired the ability of *lin-1* to be negatively regulated, because they caused strong gain-of-function phenotypes. The defect in the ability of *lin-1* to control cell fates could be caused by a defect in the ability of the mutant protein to regulate transcription, a reduced level of mutant protein caused by mRNA or protein instability, or a combination of such defects. The *n1790* nonsense mutation seems to reduce mRNA stability, which contributed to its phenotype.

Our genetic results indicate that the *lin-1(gf)* mutations result in altered *lin-1* activity. We suggest the mutant *lin-1* alleles are constitutively active in cells in which *lin-1*(+) is negatively regulated, and we propose that this ectopic activity can be used to infer the normal functions of *lin-1*. *lin-1(gf)* alleles have not been described previously, and the phenotype caused by these alleles considered together with the phenotype caused by *lin-1(lf)* alleles clarifies the functions of *lin-1*. *lin-1(lf)* mutations cause a strong Muv phenotype (Horvitz and Sulston 1980; Sulston and Horvitz 1981; Ferguson and Horvitz 1985; Ferguson *et al.* 1987; Beitel *et al.* 1995). In our experiments, *lin-1(gf)* mutations caused a weak Vul phenotype and caused P3.p, P4.p, and P8.p to adopt the nonvulval 3° fate in *let-60(gf)* mutants. These observations suggest that *lin-1* activity prevents Pn.p cells from adopting vulval fates. The *lin-1(gf)* mutations caused larval lethality characterized by a rigid, rod-like morphology. This lethality is likely to result from a failure to establish the excretory duct cell fate and hence from defective osmoregulation (Yochem *et al.* 1997). A *lin-1(lf)* mutation can suppress the larval lethality caused by a loss of activity of the RTK-Ras-MAP kinase signaling pathway (reviewed by Kornfeld 1997). These observations suggest that *lin-1* activity prevents a precursor cell from adopting the excretory duct fate. The *lin-1(gf)* mutations did not cause hermaphrodite sterility, and a *lin-1(lf)* mutation does not suppress the hermaphrodite sterility caused by a loss of the activity of the Ras-MAP kinase pathway (Kornfeld *et al.* 1995a). Thus, *lin-1* does not appear to function in the germ cells, which require the activity of the Ras-MAP kinase pathway to exit from pachytene (Church *et al.* 1995).

Genetic epistasis tests with both classes of *lin-1* alleles lead to similar conclusions about the position of *lin-1* in the signaling pathway. The *lin-1(lf)* mutation (Muv phenotype) is epistatic to a *let-60 ras* loss-of-function mutation (Vul phenotype) (Han *et al.* 1990). Similarly, the *lin-1(gf)* mutation (Vul phenotype) was epistatic to a *let-60 ras* gain-of-function mutation (Muv phenotype). Both findings suggest that *lin-1* functions downstream of *let-60 ras*, if these two genes function in a linear signaling pathway. Taken together, the genetic analyses of the *lin-1(gf)* and *lin-1(lf)* mutations strongly support the model that *lin-1* is negatively regulated by the activity of the RTK-Ras-MAP kinase pathway to allow the establishment of the excretory duct cell fate and allow P6.p to adopt a 1° vulval fate.

LIN-1 is likely to be phosphorylated and thereby regulated directly by ERK MAP kinase: Although genetic experiments show that *lin-1* and *mpk-1* function in the same processes, epistasis tests do not prove that *lin-1* is negatively regulated by the RTK-Ras-MAP kinase pathway, because these data are also consistent with the

possibility that *lin-1* functions in a parallel signaling pathway and is negatively regulated by other molecules. Furthermore, even if *lin-1* is negatively regulated by the RTK-Ras-MAP kinase pathway, the genetic data are consistent with either direct or indirect regulation of *lin-1* by *mpk-1* ERK MAP kinase. Here we show that murine Erk2 can phosphorylate LIN-1 *in vitro*. The K_m for full-length LIN-1 was 0.18 μm, about 18-fold lower than the K_m for myelin basic protein, showing LIN-1 is a high-affinity substrate and suggesting that phosphorylation of LIN-1 is not likely to result from promiscuous kinase activity *in vitro*. Vertebrate Erk2 was used because purified, active enzyme is readily available. However, it is likely that *C. elegans* MPK-1 also can phosphorylate LIN-1, since *C. elegans mpk-1* shares more than 70% identity with vertebrate ERK, and vertebrate ERK can functionally substitute for *C. elegans mpk-1* (Lackner *et al.* 1994; Wu and Han 1994). Taken together, the genetic experiments suggesting that *mpk-1* ERK MAP kinase functions upstream of *lin-1* at multiple times during development and the biochemical demonstration that Erk2 can phosphorylate LIN-1 strongly support the model that MPK-1 phosphorylation directly regulates LIN-1. This model predicts that LIN-1 is phosphorylated *in vivo* and that phosphorylation requires *mpk-1*. We are testing these predictions.

We have not yet determined the precise LIN-1 residues that are phosphorylated by ERK. However, we found that the C-terminal 160 residues were necessary for phosphorylation of full-length LIN-1 and sufficient to function as an Erk2 substrate, suggesting that phosphorylation of full-length LIN-1 occurs in this region. Furthermore, each *lin-1(gf)* mutation is predicted to affect the C terminus of LIN-1 and these alleles appear to be constitutively active, suggesting the C terminus is necessary for LIN-1 to be negatively regulated. These findings support the model that MAP kinase phosphorylation of the LIN-1 C terminus causes negative regulation of LIN-1 activity. We have not determined how phosphorylation regulates LIN-1. Phosphorylation might decrease LIN-1 protein activity or result in a change in protein localization or stability.

The finding that LIN-1, a predicted transcription factor, is directly regulated by ERK supports the model that MAP kinase is a transition point between signaling proteins and proteins that mediate cell-fate changes. Furthermore, the finding that *lin-1* is an important target of *mpk-1* ERK MAP kinase during the establishment of the excretory duct cell fate and during vulval development but not in germ cells suggests that *mpk-1* ERK MAP kinase does not regulate the same target proteins in each developmental context. These observations support the model that MAP kinase contributes to the specificity of different cellular responses by phosphorylating different target proteins in different cells. LIN-1 is the first *C. elegans* protein shown to be directly regulated by ERK MAP kinase, and many important questions about specificity remain to be answered. For example, how many different proteins are phosphorylated by *mpk-1* ERK MAP kinase *in vivo*, how much overlap exists between *mpk-1* ERK MAP kinase targets in different cells, and is target specificity controlled by target protein availability and/or differences in *mpk-1* ERK MAP kinase in different cells?

***C. elegans* LIN-1, vertebrate Elk-1, SAP-1a, Net, and Drosophila Aop are members of the Elk subfamily of ETS proteins:** Conserved structure and conserved function can be used to infer the evolutionary relationships among *ets* genes. We propose that LIN-1 and Drosophila Aop are members of the Elk subfamily, which contains the vertebrate proteins Elk-1, SAP-1a, and Net/ERP/SAP-2 (Giovane *et al.* 1994; Treisman 1994). This model is supported by three similarities among these proteins—sequence and position of the ETS domain, sequence and position of the C box, and interactions with ERK. Other ETS proteins do not share all of these features, although a few ETS proteins share some of these features. The structural and sequence similarities are described in results and illustrated in Figure 3.

All five proposed members of the Elk subfamily appear to be phosphorylated by ERK. Elk-1, SAP-1a, and Net are ternary complex factors that bind the serum response element present in the promoters of immediate early genes, such as *c-fos* (reviewed by Treisman 1994). In cultured vertebrate cells, transcription of immediate early genes is rapidly induced by activation of RTK-Ras-ERK MAP kinase pathways. This induction seems to be mediated by phosphorylation of ternary complex factors. *In vitro*, ERK phosphorylates multiple sites in and around the Elk-1 C box; the same sites are phosphorylated *in vivo* following activation of the Ras-ERK MAP kinase pathway (Janknecht *et al.* 1993; Marais *et al.* 1993). Phosphorylation stimulates the ability of the Elk-1 C terminus to function as a transcriptional activation domain. The C termini of SAP-1a and Net behave like the C terminus of Elk-1 (Price *et al.* 1995). Genetic analysis shows that *aop* is an important regulator of cell-fate decisions at multiple times during Drosophila development (Lai and Rubin 1992). *aop* appears to be negatively regulated by RTK-Ras-ERK MAP kinase pathways in flies and in cultured Drosophila cells (O'Neill *et al.* 1994). Aop can be phosphorylated by ERK *in vitro* (Brunner *et al.* 1994). In flies mutant versions of Aop that lack multiple putative MAP kinase phosphorylation sites are unresponsive to negative regulation (Rebay and Rubin 1995). Phosphorylation may cause Aop protein to leave the nucleus and be degraded (Rebay and Rubin 1995). Genetic analyses suggest *lin-1* is negatively regulated by RTK-Ras-ERK MAP kinase pathways, and our biochemical experiments suggest the mechanism is phosphorylation of the C terminus by ERK. These observations suggest *lin-1*, *aop*, *elk-1*, *sap-1*, and *net* are derived from a common ancestral gene that encoded a protein that was phosphorylated by ERK MAP

kinase. The findings that phosphorylation positively regulates Elk-1 but negatively regulates LIN-1 and Aop suggest that the effect of ERK phosphorylation has diverged during evolution.

FQFP may be a recognition motif for ERK MAP kinases: MAP kinases can be divided into subfamilies based on particular conserved residues; five subfamilies are currently known in budding yeast and three in vertebrates (reviewed by Davis 1995; Treisman 1996). *C. elegans* MPK-1, Drosophila ERKA, and vertebrate Erk-1 and Erk-2 are members of the ERK MAP kinase subfamily (Lackner *et al.* 1994; Treisman 1996). All MAP kinases phosphorylate SP and TP motifs (reviewed by Davis 1993). However, 90% of all proteins have one or more S/TP sequences (data not shown), and yet a particular MAP kinase does not phosphorylate all these proteins or every S/TP sequence within a target protein. The mechanisms that achieve target specificity have not been established.

We propose, based upon three pieces of evidence, that FQFP is a recognition motif that enables substrate proteins to bind ERK MAP kinase. First, FQFP is a conserved element of the C box. Comparisons of Elk-1, SAP-1a, and Net first identified the C box as a region with extensive sequence conservation (Giovane *et al.* 1994; Treisman 1994). Our analysis revealed that LIN-1 and Aop contain divergent C boxes, and the only highly conserved elements among all these C boxes are multiple S/TP sequences and the FQFP motif. The S/TP sequences in the C boxes of Elk-1 and SAP-1a are the major phosphorylation sites for ERK (Janknecht *et al.* 1993; Janknecht and Hunter 1997; Marais *et al.* 1993). The conservation of the FQFP motif and its proximity to crucial phosphorylation sites implicates the FQFP motif in this process. Second, our results suggest that changing the FQFP motif affects the regulation of LIN-1 *in vivo*. The proteins encoded by *lin-1(n2515)* and *lin-1(n2525)* have a change in the proline of the FQFP motif and appear to be partially unresponsive to negative regulation by the RTK-Ras-MAP kinase pathway. The proteins encoded by *lin-1(n1790)* and *lin-1(n1761)* lack the FQFP motif and appear to be extremely unresponsive to negative regulation. We propose that these mutant proteins are constitutively active because alterations in the FQFP motif prevent efficient recognition and phosphorylation by MPK-1 ERK MAP kinase. Third, our *in vitro* biochemical experiments support this hypothesis. GST:LIN-1(1–441P384L), which has the amino acid substitution caused by *lin-1(n2515)*, had a K_m for Erk2 that was fourfold higher than the K_m of wild-type LIN-1. GST:LIN-1(1–379), which lacks the FQFP motif and is similar to the mutant protein encoded by *n1761*, had a K_m for Erk2 that was sixfold higher than the K_m of full-length LIN-1. Thus, the severity of the change in the FQFP motif correlates with the ability of LIN-1 to be phosphorylated by Erk2 *in vitro* and the ability of *lin-1* to be negatively regulated *in vivo*.

The role of the FQFP sequence in Elk-1, SAP-1a, and Net or the FQFHP sequence in Aop has not been investigated directly. However, the aop^{yanS2382} mutation is a 5 bp deletion that shifts the reading frame, thereby replacing the C-terminal 162 amino acids with a new group of 86 amino acids (Rebay and Rubin 1995); the mutant Aop protein lacks the FQFHP motif and some S/TP sequences (Figure 3) and thus resembles the proteins encoded by *lin-1(n1790)* and *lin-1(n1761)*. Genetic analysis also indicates that aop^{yanS2382} resembles the *lin-1(gf)* alleles, since aop^{yanS2382} was isolated in a genetic screen for suppressors of activated Ras and it appears to be unresponsive to Ras-MAP kinase signaling, which negatively regulates *aop*(+) (Rebay and Rubin 1995; Karim *et al.* 1996). We propose that this mutant Aop protein is not phosphorylated efficiently by ERK, because it lacks the recognition motif and is therefore constitutively active. We are now performing biochemical experiments to test the role of the FQFP motif in mediating ERK MAP kinase target recognition.

We thank Cheri Zobel and Radhika Tripuraneni for scoring *lin-1* phenotypes, Andrew Turk and Danielle Glossip for constructing *lin-1* expression plasmids, and Jennie Liang and Yunxiang Zhu for guidance about protein analysis. Some strains were provided by the Caenorhabditis Genetics Center (St. Paul, MN), which is supported by the National Institutes of Health. This research was in part supported by the Edward Mallinckrodt, Jr. Foundation (K.K.). H.R.H. is an Investigator and G.J.B. was a predoctoral fellow of the Howard Hughes Medical Institute.

LITERATURE CITED

Alessi, D. R., P. Cohen, A. Ashworth, S. Cowley, S. J. Leevers *et al.*, 1995 Assay and expression of mitogen-activated protein kinase, MAP kinase kinase, and Raf. Methods Enzymol. **255:** 279–290.

Beitel, G. J., S. G. Clark and H. R. Horvitz, 1990 *Caenorhabditis elegans ras* gene *let-60* acts as a switch in the pathway of vulval induction. Nature **348:** 503–509.

Beitel, G. J., S. Tuck, I. Greenwald and H. R. Horvitz, 1995 The *Caenorhabditis elegans* gene *lin-1* encodes an ETS-domain protein and defines a branch of the vulval induction pathway. Genes Dev. **9:** 3149–3162.

Brenner, S. 1974 The genetics of *Caenorhabditis elegans.* Genetics **77:** 71–94.

Brunner, D., K. Ducker, N. Oellers, E. Hafen, H. Scholz *et al.*, 1994 The ETS domain protein Pointed-P2 is a target of MAP kinase in the Sevenless signal transduction pathway. Nature **370:** 386–389.

Church, D. L., K.-L. Guan and E. J. Lambie, 1995 Three genes of the MAP kinase cascade, *mek-2, mpk-1/sur-1* and *let-60 ras*, are required for meiotic cell cycle progression in *Caenorhabditis elegans.* Development **121:** 2525–2535.

Clark, S. G., M. J. Stern and H. R. Horvitz, 1992 *C. elegans* cell-signaling gene *sem-5* encodes a protein with SH2 and SH3 domains. Nature **356:** 340–344.

Clark, S. G., A. D. Chisholm and H. R. Horvitz, 1993 Control of cell fates in the central body region of C. elegans by the homeobox gene *lin-39.* Cell **74:** 43–55.

Coulondre, C., and J. H. Miller, 1977 Genetic studies of the *lac* repressor. IV. Mutagenic specificity in the *LacI* gene of *Escherichia coli.* J. Mol. Biol. **117:** 577–606.

Dalton, S., and R. Treisman, 1992 Characterization of SAP-1, a protein recruited by serum response factor to the c-*fos* serum response element. Cell **68:** 597–612.

Davis, R. J., 1993 The mitogen-activated protein kinase signal transduction pathway. J. Biol. Chem. **268:** 14553–14556.

Davis, R. J., 1995 Transcriptional regulation by MAP kinases. Mol. Reprod. Dev. **42:** 459–467.

Dickson, B., and E. Hafen, 1994 Genetics of signal transduction in invertebrates. Curr. Opin. Genet. Dev. **4:** 64–70.

Ferguson, E. L., and H. R. Horvitz, 1985 Identification and characterization of 22 genes that affect the vulval cell lineages of the nematode *Caenorhabditis elegans.* Genetics **110:** 17–72.

Ferguson, E. L., P. W. Sternberg and H. R. Horvitz, 1987 A genetic pathway for the specification of the vulval cell lineages of *Caenorhabditis elegans.* Nature **326:** 259–267.

Giovane, A., P. Alexander, S.-M. Maira, P. Sobieszczuk and B. Wasylyk, 1994 Net, a new *ets* transcription factor that is activated by Ras. Genes Dev. **8:** 1502–1513.

Han, M., R. V. Aroian and P. W. Sternberg, 1990 The *let-60* locus controls the switch between vulval and nonvulval cell fates in *Caenorhabditis elegans.* Genetics **126:** 899–913.

Han, M., A. Golden, Y. Han and P. W. Sternberg, 1993 *C. elegans lin-45 raf* gene participates in *let-60 ras*-stimulated vulval differentiation. Nature **363:** 133–140.

Horvitz, H. R., and P. W. Sternberg, 1991 Multiple intercellular signalling systems control the development of the *Caenorhabditis elegans* vulva. Nature **351:** 535–541.

Horvitz, H. R., and J. E. Sulston, 1980 Isolation and genetic characterization of cell lineage mutants of the nematode *Caenorhabditis elegans.* Genetics **96:** 435–454.

Janknecht, R., and T. Hunter, 1997 Convergence of MAP kinase pathways on the ternary complex factor Sap-1a. EMBO J. **16:** 1620–1627.

Janknecht, R., W. H. Ernst, V. Pingoud and A. Nordheim, 1993 Activation of ternary complex factor Elk-1 by MAP kinase. EMBO J. **12:** 5097–5104.

Karim, F. D., H. C. Chang, M. Therrien, D. A. Wassarman, T. Laverty *et al.*, 1996 A screen for genes that function downstream of Ras1 during Drosophila eye development. Genetics **143:** 315–329.

Kornfeld, K., 1997 Vulval development in *Caenorhabditis elegans.* Trends Genet. **13:** 55–61.

Kornfeld, K., K.-L. Guan and H. R. Horvitz, 1995a The *Caenorhabditis elegans* gene *mek-2* is required for vulval induction and encodes a protein similar to the protein kinase MEK. Genes Dev. **9:** 756–768.

Kornfeld, K., D. B. Hom and H. R. Horvitz, 1995b The *ksr-1* gene encodes a novel protein kinase involved in Ras-mediated signaling in C. elegans. Cell **83:** 903–913.

Lackner, M. L., K. Kornfeld, L. M. Miller, H. R. Horvitz and S. K. Kim, 1994 A MAP kinase homolog, *mpk-1*, is involved in *ras*-mediated induction of vulval cell fates in *Caenorhabditis elegans.* Genes Dev. **8:** 160–173.

Lai, Z.-C., and G. M. Rubin, 1992 Negative control of photoreceptor development in Drosophila by the product of the *yan* gene, an ETS domain protein. Cell **70:** 609–620.

Marais, R., J. Wynne and R. Treisman, 1993 The SRF accessory protein Elk-1 contains a growth factor-regulated transcriptional activation domain. Cell **73:** 381–393.

Miller, L. M., M. E. Gallegos, B. A. Morrisseau and S. K. Kim, 1993 *lin-31*, a *Caenorhabditis elegans* HNF-3/*fork head* transcription factor homolog, specifies three alternative cell fates in vulval development. Genes Dev. **7:** 933–947.

O'Neill, E. M., I. Rebay, R. Tijan and G. M. Rubin, 1994 The activities of two Ets-related transcription factors required for Drosophila eye development are modulated by the Ras/MAPK pathway. Cell **78:** 137–147.

Price, M. A., A. E. Rogers and R. Treisman, 1995 Comparative analysis of the ternary complex factors Elk-1, SAP-1a and SAP-2 (ERP/NET). EMBO J. **14:** 2589–2601.

Pulak, R., and P. Anderson, 1993 mRNA surveillance by the *Caenorhabditis elegans smg* genes. Genes Dev. **7:** 1885–1897.

Rao, V. N., K. Huebner, I. Masaharu, A. ar-Rushdi, C. M. Croce *et al.*, 1989 *elk*, tissue-specific *ets*-related genes on chromosomes X and 14 near translocation breakpoints. Science **244:** 66–70.

Rebay, I., and G. M. Rubin, 1995 Yan functions as a general inhibitor of differentiation and is negatively regulated by activation of the Ras1/MAPK pathway. Cell **81:** 857–866.

Riddle, D. L., T. Blumenthal, B. J. Meyer and J. R. Priess (Editors), 1997 *C. elegans II*. Cold Spring Harbor Laboratory Press, Cold Spring Harbor, NY.

Rogalski, T. M., and D. L. Riddle, 1988 A *C. elegans* RNA polymerase II gene, *ama-1* IV, and nearby essential genes. Genetics **118:** 61–74.

Sambrook, J., E. F. Fritsch and T. Maniatis, 1989 *Molecular Cloning: A Laboratory Manual*, Ed. 2, Cold Spring Harbor Laboratory Press, Cold Spring Harbor, NY.

Sulston, J. E., and H. R. Horvitz, 1977 Post-embryonic cell lineages of the nematode, *Caenorhabditis elegans.* Dev. Biol. **56:** 110–156.

Sulston, J. E., and H. R. Horvitz, 1981 Abnormal cell lineages in mutants of the nematode *Caenorhabditis elegans.* Dev. Biol. **82:** 41–55.

Sundaram, M., and M. Han, 1995 The C. elegans *ksr-1* gene encodes a novel Raf-related kinase involved in Ras-mediated signal transduction. Cell **83:** 889–901.

Sundaram, M., and M. Han, 1996 Control and integration of cell signaling during *C. elegans* vulval development. Bioessays **18:** 473–480.

Traub, L. M., J. A. Ostrom and S. Kornfeld, 1993 Biochemical dissection of AP-1 recruitment onto Golgi membranes. J. Cell Biol. **123:** 561–573.

Treisman, R., 1994 Ternary complex factors: growth factor regulated transcriptional activators. Curr. Opin. Genet. Dev. **4:** 96–101.

Treisman, R., 1996 Regulation of transcription by MAP kinase cascades. Curr. Opin. Cell Biol. **8:** 205–215.

Wasylyk, B., S. L. Hahn and A. Giovane, 1993 The Ets family of transcription factors. Eur. J. Biochem. **211:** 7–18.

Williams, B. D., B. Schrank, C. Huynh, R. Shownkeen and R. H. Waterston, 1992 A genetic mapping system in *Caenorhabditis elegans* based on polymorphic sequence-tagged sites. Genetics **131:** 609–624.

Wu, Y., and M. Han, 1994 Suppression of activated Let-60 Ras protein defines a role of *Caenorhabditis elegans* Sur-1 MAP kinase in vulval differentiation. Genes Dev. **8:** 147–159.

Yochem, J., M. Sundaram and M. Han, 1997 Ras is required for a limited number of cell fates and not for general proliferation in *Caenorhabditis elegans.* Mol. Cell. Biol. **17:** 2716–2722.

Communicating editor: I. Greenwald